Nonlinear approximation theory for the homogeneous Boltzmann equation III

Minh-Binh Tran
Department of Mathematics
University of Wisconsin Madison
Email: mtran23@wisc.edu

October 29, 2017

Abstract

The current paper is the third part of our work on the nonlinear approximation theory for the homogeneous Boltzmann equation. In the first two parts, we introduced an adaptive, non-truncated wavelet spectral method for the numerical resolution of the equation. A convergence theory and a wavelet filtering technique to preserve some physical properties of the solution were also provided. In this part of the work, we give an explicit formulation of the algorithm in the concrete case of the Haar wavelet. We also provide numerical tests to confirm the theoretical results done in the previous parts of the work.

Keyword Boltzmann equation, wavelet, adaptive spectral method, Maxwell lower bound, nonlinear approximation theory, numerical stability, wavelet filter.
MSC: 82C40, 65M70, 76P05, 41A46, 42C40.

Contents

1 Introduction

The Boltzmann equation describes the behaviour of a dilute gas of particles when only the binary elastic collisions are considered. In this work, we are interested in the numerical resolution of the space homogeneous Boltzmann equation

$$\frac{\partial f}{\partial t} = Q(f, f), \quad v \in \mathbb{R}^d, \tag{1.1}$$

where $f := f(t, v)$ is the time-dependent particle distribution function for the phase space. The quadratic Boltzmann collision operator Q is a defined

$$Q(f, f)(v) = \int_{\mathbb{R}^d} \int_{\mathbb{S}^{d-1}} B(|v - v_*|, \cos\theta)(f'_* f' - f_* f) d\sigma dv_*, \tag{1.2}$$

where $f = f(v)$, $f_* = f(v_*)$, $f' = f(v')$, $f'_* = f(v'_*)$ and

$$\begin{cases} v' = v - \frac{1}{2}((v - v_* - |v - v_*|\sigma), \\ v'_* = v - \frac{1}{2}((v - v_* + |v - v_*|\sigma), \end{cases}$$

with $\sigma \in \mathbb{S}^{d-1}$.
We assume that

$$B(|u|, \cos\theta) = |u|^\gamma b(\cos\theta), \qquad \cos\theta = \left\langle \frac{v - v_*}{|v - v_*|}, \sigma \right\rangle, \tag{1.3}$$

where $\gamma \in [0, 1]$ and b is a smooth function satisfying

$$\int_0^\pi b(\cos\theta) \sin\theta d\theta < +\infty, \tag{1.4}$$

and assumptions (2.1)-(2.2) in [18]

$$\exists \theta_b > 0 \text{ such that } supp\{b(\cos\theta)\} \subset \{\theta \quad | \quad \theta_b \leq \theta \leq \pi - \theta_b\}. \tag{1.5}$$

Under these assumptions, the collision operator could be split as

$$Q(f, f) = Q^+(f, f) - L(f)f,$$

with

$$Q^+(f,f) = \int_{\mathbb{R}^3}\int_{\mathbb{S}^2} B(|v-v_*|,\cos\theta) f'_* f' d\sigma dv_*$$

and

$$L(f) = \int_{\mathbb{R}^3}\int_{\mathbb{S}^2} B(|v-v_*|,\cos\theta) f_* d\sigma dv_*.$$

Boltzmann collision operator has the properties of conserving mass, momentum and energy

$$\int_{\mathbb{R}^d} Q(f,f)dv = 0, \quad \int_{\mathbb{R}^d} Q(f,f)vdv = 0, \quad \int_{\mathbb{R}^d} Q(f,f)|v|^2 dv = 0,$$

and it satisfies the Boltzmann's H-theorem

$$-\frac{d}{dt}\int_{\mathbb{R}^d} f\log f dv = -\int_{\mathbb{R}^d} Q(f,f) log f dv \geq 0,$$

in which $-\int f\log f$ is the *entropy* of the solution. The Boltzmann's H-theorem implies that any equilibrium distribution function has the form of a Maxwellian distribution

$$M(\rho,u,T) = \frac{\rho}{(2\pi T)^{3/2}}\exp\left(-\frac{|u-v|^2}{2T}\right),$$

where ρ, u, T are the *density, macroscopic velocity* and *temperature* of the gas

$$\rho = \int_{\mathbb{R}^d} f(v)dv, \quad u = \frac{1}{\rho}\int_{\mathbb{R}^d} vf(v)dv, \quad T = \frac{1}{3\rho}\int_{\mathbb{R}^d} |u-v|^2 f(v)dv.$$

We suppose that the initial datum f_0 is positive on $\mathbb{R}^{2d}$ and

$$\int_{\mathbb{R}^d} f_0(v)(1+|v|^2)dv < +\infty.$$

We refer to [7] and [27] for further details and discussions on the Boltzmann equation.

The numerical resolution of the Boltzmann equation has a very important role in the study of the kinetic theory of gases. Several strategies have been proposed to discretize the multidimensional Boltzmann collision operator. One of the first natural approaches is the Monte Carlo method, introduced in [2]. The method produces very good approximation of the solution of the equation, but it is quite expensive. Among other approaches, Discrete

Velocity Models - VDMs ([6, 4, 3, 19]) is an efficient deterministic technique based on a Cartesian grid in velocity and a discrete collision operator, which is a nonlinear system of conservation laws. DVMs were proved to be consistent ([9]) and converge weakly to the solution of the main equation ([20, 16]). The draw-back of this technique is the high cost of computation and the lack of theoretical study on the strong convergence of the solutions and error estimates of the system of conservation laws to the solution of the Boltzmann equation. Another well-known approach is the Fourier Spectral Methods - FSMs ([21, 22, 11, 10, 13, 14]). The main idea of this class of techniques is to truncate the velocity space and periodize the solution on the new bounded domain. The major drawback of DVMs and FSMs is that the velocity is approximate by a bounded region. For DVMs, the truncation breaks down the convolution structure of the collision operators. For FSMs, we need to impose nonphysical periodic boundary conditions.

In our work, we introduce a new way to deal with the truncation problem: in stead of truncating the computational domain from $\mathbb{R}^d$ into a bounded domain $(-R, R)^d$ and constructing a mesh on the truncated domain like classical deterministic approaches, we choose a change of variable mapping $\varphi : \mathbb{R}^d \to (-1, 1)^d$ and construct a nonlinear wavelet basis for $(-R, R)^d$ in the following way: Let $\{e_n\}$ be a wavelet on $L^2(-1, 1)^d$, then $e_n(\varphi)$ will be our new wavelet basis taking values on the full space $\mathbb{R}^d$. Using this new wavelet basis, we can construct a wavelet spectral method to solve Boltzmann equation numerically. If the scaling function of the wavelet basis $\{e_n\}$ is positive, we could prove that the numerical solution of the Boltzmann equation is also positive. The new wavelet basis is adaptive, in the sense that by using φ, the mesh around the origin is very fine, while the mesh away from the origin is very coarse. Since theoretical results show that the solution of the Boltzmann equation is bounded from below and above by Maxwellians ([24, 17, 12]), this particular mesh is adapted to the Boltzmann equation. Our work is divided into three parts: In the first part [25], we proved that the algorithm converges in the energy norm. In the second part [26], we introduce a filtering technique to preserve the propagation of polynomial and exponential moments of the approximate solution. Our current paper is the third part of the work, which is devoted to the practical and numerical aspects of the theory.

The plan of our paper is the following: In section 2, we construct the nonlinear wavelet basis (subsection 2.1), then build the wavelet spectral algorithm (subsection 2.2) and give a formulation of the algorithm in the concrete case of the Haar wavelet (subsection 2.3). The numerical case tests will be presented in section 3.

2 Wavelet spectral algorithm for the Boltzmann equation

2.1 Adaptive wavelet basis

Let $\bar{\phi}$ be a *positive scaling function* which defines a *multiresolution analysis*, i.e., a ladder of embedded approximation subspaces of $L^2(-1,1)$

$$V_0 \subset V_{-1} \cdots \to L^2(-1,1)$$

such that $\bar{\phi}_{j,k} = \{2^{-j/2}\phi(2^{-j}y-k)\}_{k\in\mathbb{Z}}$ constitutes an orthonormal basis for V_j. The *wavelet* ψ is built to characterize the missing details between two adjacent levels of approximation: $\{\bar{\psi}_{j,k}\}_{k\in\mathbb{Z}} = \{2^{-j/2}\bar{\psi}(2^{-j}y-k)\}_{k\in\mathbb{Z}}$ is an orthonormal basis of W_j where

$$V_{j-1} = V_j \oplus W_j.$$

Suppose that the scaling function $\bar{\phi}$ and the wavelet $\bar{\psi}$ have reasonable decays, for example $|\bar{\phi}(y)|, |\bar{\psi}(y)| \leq C(1+|y|)^{-2-\epsilon}, \epsilon > 0$. We refer to the books [8, 15] for more details on wavelets. Define the change of variables mapping:

$$\begin{aligned} &\varphi : \mathbb{R} \to (-1,1), \\ &\varphi(v) = \frac{v}{1+|v|}. \end{aligned} \tag{2.1}$$

The new nonlinear wavelet basis is then $\{\psi_{j,k}\}_{k\in\mathbb{Z}} = \{\psi_{j,k}(\varphi)\}_{k\in\mathbb{Z}}$. Notice that the Jacobian of this change of variables is $\frac{1}{(1+|v|)^2}$.

We now construct an adaptive multiresolution analysis for $L^2((-1,1)^d)$. Define

$$\Psi_{j,k}(y) = \psi_{j_1,k_1}(y_1)\ldots\psi_{j_d,k_d}(y_d),$$

and

$$\Phi_{j,k}(y) = \phi_{j_1,k_1}(y_1)\ldots\phi_{j_d,k_d}(y_d),$$

where $j = (j_1,\ldots,j_d) \in (-\mathbb{N})^d, k = (k_1,\ldots,k_d) \in \{0,\ldots,2^{|j|}-1\}^2$, $y = (y_1,\ldots,y_d) \in \mathbb{R}^d$.

Therefore, $\{\Psi_{j,k}\}$ is a wavelet basis of $L^2(\mathbb{R}^d)$ with weight

$$J(y) = (1+|y_1|)^{-2}\ldots(1+|y_d|)^{-2}. \tag{2.2}$$

Notice that our nonlinear multiresolution analysis is slightly different from the ones in [25, 26].

2.2 Wavelet spectral algorithm

Similar as in [25, 26], we construct a wavelet spectral algorithm for (1.1). We expand f using the wavelet $\{\Psi_{j,k}\}$ and take the following truncation

$$f_N = \sum_{k=(0,0)}^{(2^N-1,2^N-1)} a_{N,k}\Psi_{N,k} \tag{2.3}$$

$$=: \sum_{k=0}^{2^N-1} a_{N,k}\Psi_{N,k}, \tag{2.4}$$

in which (2.4) is defined as an abbreviation of (2.3). Equivalently, we can also use the basis created by the scaling function

$$f_N = \sum_{k=0}^{2^N-1} b_{N,k}\Phi_{N,k}. \tag{2.5}$$

Plugging (2.3) into (1.1), we get the following approximate system

$$\partial_t f_N = P_N(Q(f_N, f_N)), \tag{2.6}$$

which is

$$\begin{aligned} &\partial_t a_{N,k}\int_{\mathbb{R}^d}\Psi_{N,k}^2 J dv \qquad (2.7)\\ =\ &\sum_{l,l'=0}^{2^N-1} a_{N,l}a_{N,l'}\int_{\mathbb{R}^{2d}\times\mathbb{S}^{d-1}} B(|v-v_*|,\sigma)\left[\Psi_{N,l}(v_*')\Psi_{N,l'}(v')\right.\\ &\left.-\Psi_{N,l}(v_*)\Psi_{N,l'}(v)\right]\Psi_{N,k}(v)J(v)d\sigma dv_* dv, \quad \forall k\in\{0,\dots,2^N-1\}, \end{aligned}$$

or

$$\begin{aligned} &\partial_t b_{N,k}\int_{\mathbb{R}^d}\Phi_{N,k}^2 J dv \qquad (2.8)\\ =\ &\sum_{l,l'=0}^{2^N-1} b_{N,l}b_{N,l'}\int_{\mathbb{R}^{2d}\times\mathbb{S}^{d-1}} B(|v-v_*|,\sigma)\left[\Phi_{N,l}(v_*')\Phi_{N,l'}(v')\right.\\ &\left.-\Phi_{N,l}(v_*)\Phi_{N,l'}(v)\right]\Phi_{N,k}(v)J(v)d\sigma dv_* dv, \quad \forall k\in\{0,\dots,2^N-1\}. \end{aligned}$$

Filtering technique: Following [26], in order to preserve the Maxwellian upper bound and the propagation of polynomial moment of the solution, we

filter some components of the solution, which gives the following system, where the unknowns are $\{a_{N,k}\}$ and $\{b_{N,k}\}$

$$\begin{aligned} & \partial_t a_{N,k} \int_{\mathbb{R}^d} \Psi_{N,k}^2 J dv \qquad (2.9) \\ = & \sum_{l,l'=0}^{2^N-1-M} a_{N,l} a_{N,l'} \int_{\mathbb{R}^{2d}\times\mathbb{S}^{d-1}} B(|v-v_*|,\sigma) \left[\Psi_{N,l}(v'_*)\Psi_{N,l'}(v') \right. \\ & \left. - \Psi_{N,l}(v_*)\Psi_{N,l'}(v)\right] \Psi_{N,k}(v) J(v) d\sigma dv_* dv, \quad \forall k \in \{0,\dots,2^N-1-M\}, \end{aligned}$$

or

$$\begin{aligned} & \partial_t b_{N,k} \int_{\mathbb{R}^d} \Phi_{N,k}^2 J dv \qquad (2.10) \\ = & \sum_{l,l'=0}^{2^N-1-M} b_{N,l} b_{N,l'} \int_{\mathbb{R}^{2d}\times\mathbb{S}^{d-1}} B(|v-v_*|,\sigma) \left[\Phi_{N,l}(v'_*)\Phi_{N,l'}(v') \right. \\ & \left. - \Phi_{N,l}(v_*)\Phi_{N,l'}(v)\right] \Phi_{N,k}(v) J(v) d\sigma dv_* dv, \quad \forall k \in \{0,\dots,2^N-1-M\}, \end{aligned}$$

where M is defined:

$$M = \left[\frac{\Delta 2^N - 1}{2}\right],$$

which is the largest integer smaller than $\frac{\Delta 2^N-1}{2}$ and Δ is some constant in $(1/2, 1)$. The solution is then represented

$$\bar{f}_N = \sum_{k=0}^{2^N-M} a_{N,k}\Psi_{N,k}. \qquad (2.11)$$

Forward Euler scheme in time: To numerically resolve (2.9) and (2.10), we employ the classical forward Euler scheme in time

$$\begin{aligned} & \frac{a_{N,k}((p+1)\Delta t) - a_{N,k}(p\Delta t)}{\Delta t} \int_{\mathbb{R}^d} \Psi_{N,k}^2 J dv \qquad (2.12) \\ = & \sum_{l,l'=0}^{2^N-1-M} a_{N,l}(p\Delta t) a_{N,l'}(p\Delta t) \int_{\mathbb{R}^{2d}\times\mathbb{S}^{d-1}} B(|v-v_*|,\sigma) \left[\Psi_{N,l}(v'_*)\Psi_{N,l'}(v') \right. \\ & \left. - \Psi_{N,l}(v_*)\Psi_{N,l'}(v)\right] \Psi_{N,k}(v) J(v) d\sigma dv_* dv, \quad \forall k \in \{0,\dots,2^N-1-M\}, \end{aligned}$$

or

$$\frac{a_{N,k}((p+1)\Delta t) - a_{N,k}(p\Delta t)}{\Delta t} \int_{\mathbb{R}^d} \Phi_{N,k}^2 J dv \qquad (2.13)$$

$$= \sum_{l,l'=0}^{2^N-1-M} b_{N,l}(p\Delta t) b_{N,l'}(p\Delta t) \int_{\mathbb{R}^{2d}\times\mathbb{S}^{d-1}} B(|v-v_*|,\sigma) \left[\Phi_{N,l}(v'_*)\Phi_{N,l'}(v') - \Phi_{N,l}(v_*)\Phi_{N,l'}(v)\right] \Phi_{N,k}(v) J(v) d\sigma dv_* dv, \quad \forall k \in \{0,\dots,2^N-1-M\},$$

where Δt is the time step length and $p\Delta t$ is the time length.

2.3 Explicit Formulation in the case of Haar wavelet

In (2.12) and (2.13), we employ the Haar wavelet

$$\mathcal{H}(y) = \begin{cases} 1 \text{ for } 0 \le y \le \frac{1}{2}, \\ -1 \text{ for } -\frac{1}{2} \le y \le 0, \\ 0 \text{ otherwise .} \end{cases} \tag{2.14}$$

Restrict our attention to the case $d = 2$ and $\gamma = 0$, the coeficients of (2.12) and (2.13) could be computed explicitely.

Remark 2.1 *Notice that for the case $d = 3$, we can also obtain an explicit formulation for the coeficients of* (2.15)*, but for $\gamma = 1$. The numerical treatment of this case is the topic of a coming paper.*

Compute the 'Gain' Coefficients: By using Haar wavelet, we can compute explicitely the coeficients

$$\int_{\mathbb{R}^{2d}\times\mathbb{S}^{d-1}} B(|v-v_*|,\sigma)\Phi_{N,l}(v'_*)\Phi_{N,l'}(v')\Phi_{N,k}(v)J(v)d\sigma dv_* dv \tag{2.15}$$

in (2.12) and (2.13). In order to compute these coefficients , it is enough to approximate

$$\int_{\mathbb{R}^2} Q(G,F)\varphi J dv$$

where $F = \chi_A$, $G = \chi_B$, $\varphi = \chi_C$ being the characteristic functions of $A = [\underline{a}_1, \overline{a}_1] \times [\underline{a}_2, \overline{a}_1]$, $B = [\underline{b}_1, \overline{b}_1] \times [\underline{b}_2, \overline{b}_2]$ and $C = [\underline{c}_1, \overline{c}_1] \times [\underline{c}_2, \overline{c}_2]$. We do the following approximation

$$\int_{\mathbb{R}^2} Q(G,F)\varphi J dv = V(C)Q(G,F)(v_C)J(v_C), \tag{2.16}$$

where $V(C) = (\overline{c}_1 - \underline{c}_1)(\overline{c}_2 - \underline{c}_2)$ is the volume of C and $v_C = \left(\frac{\overline{c}_1+\underline{c}_1}{2}, \frac{\overline{c}_2+\underline{c}_2}{2}\right)$ is the center of C.

We will represent below an exact formulation for $Q(G,F)(v)$. Recall Carleman's representation

$$Q(G,F)(v) = 2\int_{\mathbb{R}^2} F(v')\frac{1}{|v-v'|}\int_{E_{v,v'}} G(v'_*)dv'_*dv',$$

where $E_{v,v}$ is the hyperplane containing v and orthogonal to $v-v'$, then

$$\begin{aligned} Q(G,F)(v) &= 2\int_{\mathbb{R}^2} \chi_A(v')\frac{1}{|v-v'|}\int_{E_{v,v'}} \chi_B(v'_*)dv'_*dv' \\ &= 2\int_{\{v'\in A\}} \frac{1}{|v-v'|}\int_{E_{v,v'}} \chi_B(v'_*)dv'_*dv' \\ &= 2\int_{\{w\in A_v\}} \frac{1}{|w|}\int_{E_{v,v'}} \chi_B(v'_*)dv'_*dw, \end{aligned}$$

where $A_v = [\underline{A}_1, \overline{A}_1]\times[\underline{A}_2,\overline{A}_1] := [\underline{a}_1 - v_1, \overline{a}_1 - v_1]\times[\underline{a}_2 - v_2, \overline{a}_1 - v_2]$. By definition, $E_{v,v'} = \{v'_*|(v'_* - v)(v-v') = 0\}$, then

$$Q(G,F)(v) = 2\int_{\{w\in A_v\}} \frac{1}{|w|}\int_{\omega.w=0} \chi_{B_v}(\omega)d\omega dw,$$

where $B_v = [\underline{B}_1, \overline{B}_1]\times[\underline{B}_2,\overline{B}_1] := [\underline{b}_1 - v_1, \overline{b}_1 - v_1]\times[\underline{b}_2 - v_2, \overline{b}_1 - v_2]$.
It is well-known in classical geometry [1, 5, 28] that

$$\begin{aligned} Q(G,F)(v) &= 2\int_{\{w\in A_v\}} \frac{1}{|w|}\int_{\omega.w=0} \chi_{B_v}(\omega)d\omega dw \qquad (2.17) \\ &= \int_{\{w\in A_v\}} \frac{1}{w_1w_2}(|w_1\overline{B}_1 + w_2\overline{B}_2| + |w_1\underline{B}_1 + w_2\underline{B}_2| \\ &\quad -|w_1\overline{B}_1 + w_2\underline{B}_2| - |w_1\underline{B}_1 + w_2\overline{B}_2|)dw. \end{aligned}$$

In order to evaluate (2.17), it is enough to employ the following formulas in the code:

$$\int_{\mathfrak{c}}^{\mathfrak{d}}\int_{\mathfrak{a}}^{\mathfrak{b}} \frac{|w_1m + w_2n|}{w_1w_2}dw_1dw_2 = \int_{m\mathfrak{c}}^{m\mathfrak{d}}\int_{n\mathfrak{a}}^{n\mathfrak{b}} \frac{|w_1+w_2|}{w_1w_2}dw_1dw_2, \qquad (2.18)$$

for $m.n\neq 0$, $\mathfrak{a},\mathfrak{b},\mathfrak{c},\mathfrak{d},m,n\in\mathbb{R}$ and

$$\begin{aligned} &\int_{\mathfrak{c}}^{\mathfrak{d}}\int_{\mathfrak{a}}^{\mathfrak{b}} \frac{|w_1+w_2|}{w_1w_2}dw_1dw_2 \\ &= 2(|\mathfrak{d}+\mathfrak{b}| + |\mathfrak{c}+\mathfrak{a}| - |\mathfrak{c}+\mathfrak{b}| - |\mathfrak{d}+\mathfrak{a}|) + \end{aligned}$$

$$
\begin{aligned}
&+log|\mathfrak{b}|[(\mathfrak{d}-\mathfrak{b})sign(\mathfrak{d}+\mathfrak{b})-(\mathfrak{c}-b)sign(\mathfrak{c}+\mathfrak{b})]\\
&-log|\mathfrak{a}|[(\mathfrak{d}-\mathfrak{a})sign(\mathfrak{d}+\mathfrak{a})-(\mathfrak{c}-\mathfrak{a})sign(\mathfrak{c}+\mathfrak{a})]\\
&+log|\mathfrak{d}|[(\mathfrak{b}-\mathfrak{d})sign(\mathfrak{d}+\mathfrak{b})-(\mathfrak{a}-\mathfrak{d})sign(\mathfrak{d}+\mathfrak{a})]\\
&-log|\mathfrak{c}|[(\mathfrak{b}-\mathfrak{c})sign(\mathfrak{b}+\mathfrak{c})-(\mathfrak{a}-\mathfrak{c})sign(\mathfrak{a}+\mathfrak{c})], \qquad (2.19)
\end{aligned}
$$

for $\mathfrak{ab}>0$, $\mathfrak{cd}>0$, $\mathfrak{a},\mathfrak{b},\mathfrak{c},\mathfrak{d},m,n\in\mathbb{R}$.

Compute the 'Loss' Coefficients: It is not so difficult to compute the loss parts in (2.12) and (2.13).

$$
\int_{\mathbb{R}^4\times\mathbb{S}}\Phi_{N,l}(v_*)\Phi_{N,l'}(v)\Phi_{N,k}(v)J(v)d\sigma dv_*dv=0,
$$

for $l'\neq k$ and

$$
\begin{aligned}
&\int_{\mathbb{R}^4\times\mathbb{S}}B(|v-v_*|,\sigma)\Phi_{N,l}(v_*)\Phi_{N,k}(v)\Phi_{N,k}(v)J(v)d\sigma dv_*dv\\
=\;& 2\pi\|\Phi_{N,l}\|_{L^1(\mathbb{R}^2)}\|\Phi_{N,k}\sqrt{J}\|^2_{L^2(\mathbb{R}^2)}.
\end{aligned}
$$

3 Numerical Results

3.1 Test 1: Two Gaussian Initial Condition

We take $b=b_0=\frac{1}{3\pi}$ and the initial condition to be the sum of two Gaussian

$$
f_0(v_1,v_2)=0.3e^{-10((v_1-1/2)^2+v_2^2)}+0.3e^{-10((v_1+1/2)^2+v_2^2)}. \qquad (3.1)
$$

The expected equilibrium should be

$$
0.15e^{-1.3(v_1^2+v_2^2)}.
$$

We take 25 mesh points in each direction, corresponding to

$$
-2.4343,-1.8531,-1.4410,-1.1333,-0.8947,-0.7043,-0.5487,-0.4191,
$$

$$
-0.3096,-0.2158,-0.1346,-0.0635,0,0.0635,0.1346,0.2158,0.3096,
$$

$$
0.4191,0.5487,0.7043,0.8947,1.1333,1.4410,1.8531,2.4343.
$$

This mesh is adaptive: it is very fine around 0 and very coarse away from 0. The distance between the two last grid points is large $2.4343-1.8531=0.5812$. This is reasonable since the solution of the equation is mainly concentrated around $(-1.4410,1.4410)$. In this case, we filter the mesh and stop the grids at the two points -2.4343 and 2.4343. However, we could stop the

grids at further grid points with coarser meshes.
In Figure 1, we plot the solution f of the equation with respect to time 1, 14, 28,42, 56, 71. In Figure 2, we plot the values of $f(t, v_1, 0)$ in time $T = 1, 5, 10, 15, 20, 25$. In both pictures the solution is positive and converges to the equilibrium state.

3.2 Test 2: BKW solution

We take $b = b_0 = \frac{1}{6\pi}$ and the initial condition to be

$$f_0(v_1, v_2) = \frac{v_1^2 + v_2^2}{5\pi(\pi/5.5)^2} e^{-\frac{v_1^2+v_2^2}{(\pi/5.5)^2}}, \tag{3.2}$$

and the exact solution of the homogeneous Boltzmann equation (1.1) is known to be

$$f(t, v_1, v_2) = \frac{1}{10\pi S^2}\left(2S - 1 + \frac{1-S}{2S}\frac{v_1^2 + v_2^2}{(\pi/5.5)^2} e^{-\frac{v_1^2+v_2^2}{2S(\pi/5.5)^2}}\right),$$

where

$$S(t) = 1 - e^{-(\pi/5.5)^2 t/30}/2.$$

We take 27 mesh points in each direction, corresponding to

$$-2.6364, -2.0210, -1.5846, -1.2588, -1.0062, -0.8045,$$

$$-0.6398, -0.5026, -0.3867, -0.2874, -0.2013, -0.1261,$$

$$-0.0597, 0, 0.0597, 0.1261, 0.2013, 0.2874,$$

$$0.3867, 0.5026, 0.6398, 0.8045, 1.0062, 1.2588,$$

$$1.5846, 2.0210, 2.6364.$$

Similar as in Test 1, it is very fine around 0 and very coarse away from 0. The distance between the two last grid points is large $2.6364 - 2.0210 = 0.6154$. Notice again that, we filter the mesh and stop the grids at the two points -2.6364 and 2.6364; but we could stop the grids at further grid points with coarser meshes.
In Figure 3, we plot the solution at time 1, 3 and 161. The numerical solution is positive and converges to the equilibrium. Figure 3d is the evolution in time of the entropy, which is decreasing and tends to the steady state as time goes to infinity.

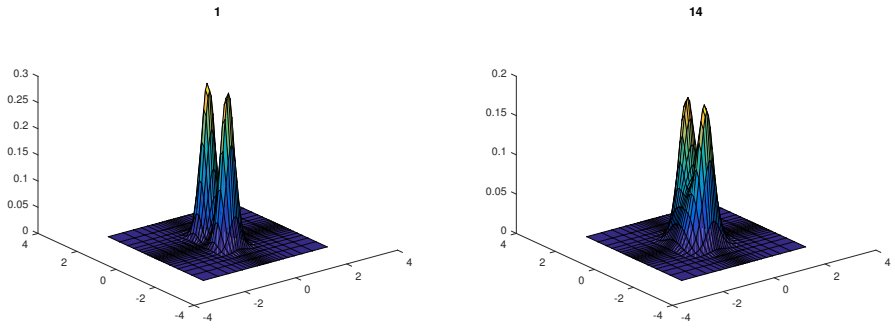

(a) $T = 1$

(b) $T = 14$

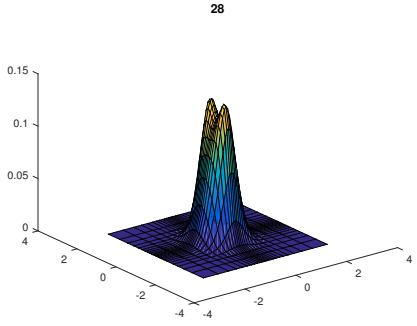

(c) $T = 28$

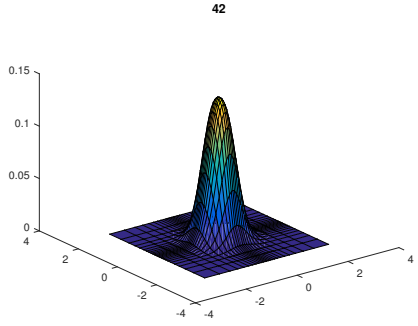

(d) $T = 42$

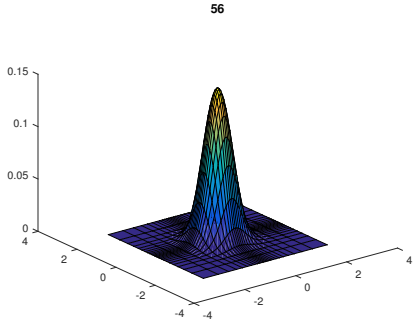

(e) $T = 56$

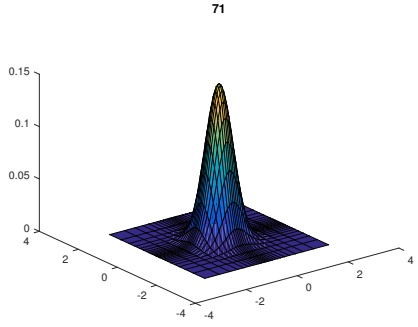

(f) $T = 71$

Figure 1: Test 1: Solution with respect to the initial data (3.1) at time 1, 14, 28,42, 56, 71

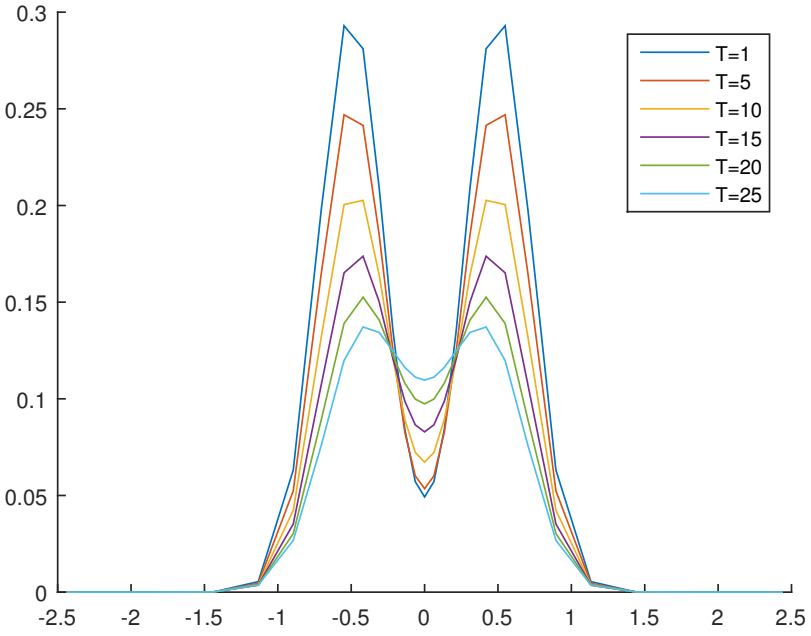

Figure 2: Test 1: Solution with respect to the initial data (3.1) at time 1, 5, 10, 15, 20, 25

The purpose of the simulations of Figure 4 is to compare the numerical solution and the exact one given by the BKW formula. We plot the numerical and exact values of $f(t, v_1, 0)$ when $T = 1, 15, 30, 45, 60$. The numerical values are denoted by triangles and the exact ones are lines. The numerical and exact solutions are on top of each other, though the mesh is coarse. The accuracy is $O(10^{-6})$.
In the simulations of Figure 5, we compare the physical quantities of the exact and computed solutions. Figure 5 is the evolution in time of the computed mass, energy and momentum, in comparison with the exact quantities. It is proved in the theoretical parts of our work (see [26]) that once the filtering technique is applied, the computed mass and energy is decreasing. On this picture, the those computed quantities could be seen to slightly decrease in time. Postprocessing techniques like the ones introduced in [13, 14] could potentially be combined with our method to prevent the loss of mass and energy.

4 Conclusion

In this paper, we complete the third part of our work on the nonlinear approximation theory for the homogeneous Boltzmann equation. We give an explicit formulation and numerical simulations for our new adaptive spectral technique to illustrate our theory developed in the first two parts of the work [25, 26]. In the first numerical test, we consider an initial data which is the sum of two Gaussian. In the second one, we compare the numerical solution with the exact solution in the BKW case. In both cases, the numerical solutions seem to provide good approximations of the exact solutions. The complexity of the algorithm is N^2, and acceleration of the method as well as the treatment of more complicated collision kernels in higher dimensions is the topic of our ongoing work. We are also trying to employ postprocessing techniques like the ones introduced in [13, 14] to improve the performance of our code.
Acknowledgements. The author would like to thank Professor Shi Jin for discussions on the topic. The author has been supported by NSF Grant RNMS (Ki-Net) 1107444, Grant MTM2011-29306-C02-00, MICINN, Spain, ERC Advanced Grant FP7-246775 NUMERIWAVES, and Grant PI2010-04 of the Basque Government.

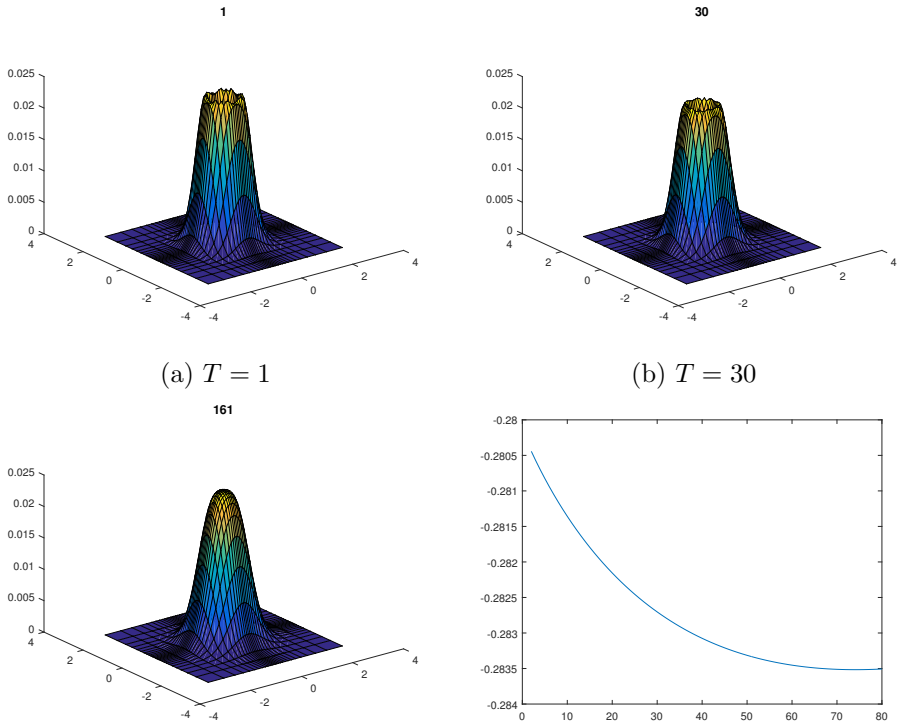

(a) $T = 1$ (b) $T = 30$

(c) $T = 161$ (d) Entropy

Figure 3: Test 2: Solution with respect to the initial data (3.2) at time 1, 30, 161 and evolution in time of the entropy

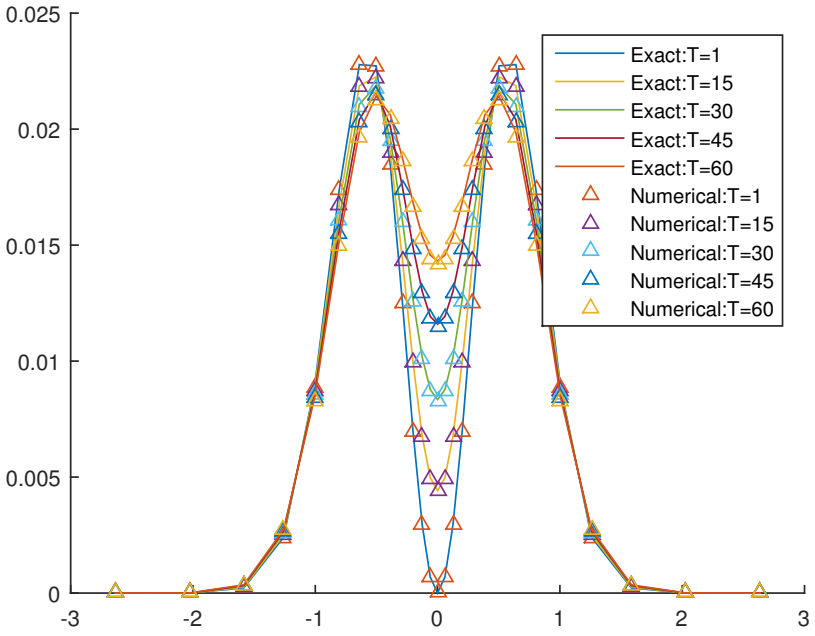

Figure 4: Test 2: Solution with respect to the initial data (3.2) at time 1, 15, 20, 35, 45, 60. The numerical solution predicts well the exact solution one, though the mesh is coarse.

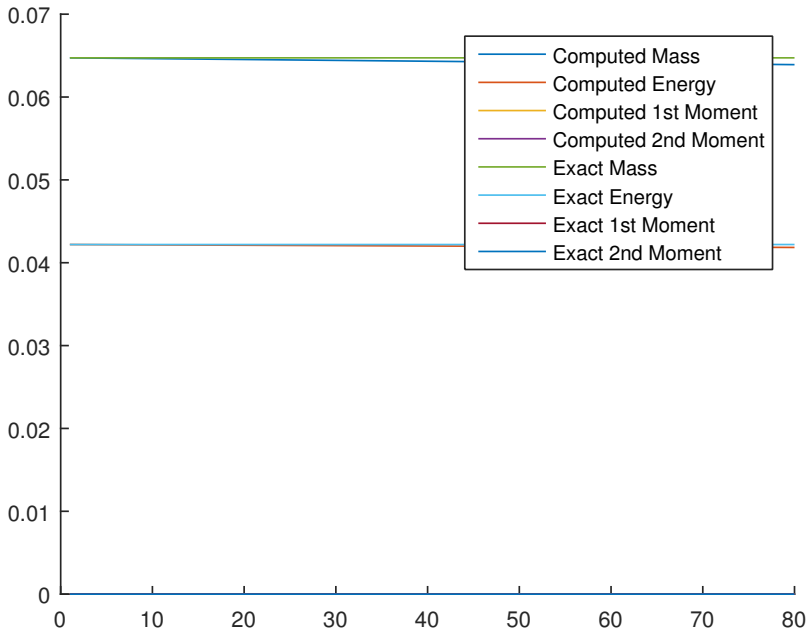

Figure 5: Test 2: Evolution in time of mass, momentum, energy, entropy in comparison with the exact quantities

References

[1] Marcel Berger. *Geometry revealed*. Springer, Heidelberg, 2010. A Jacob's ladder to modern higher geometry, Translated from the French by Lester Senechal.

[2] G. A. Bird. *Molecular gas dynamics and the direct simulation of gas flows*, volume 42 of *Oxford Engineering Science Series*. The Clarendon Press Oxford University Press, New York, 1995. Corrected reprint of the 1994 original, With 1 IBM-PC floppy disk (3.5 inch; DD), Oxford Science Publications.

[3] Alexander V. Bobylev and Carlo Cercignani. Discrete velocity models without nonphysical invariants. *J. Statist. Phys.*, 97(3-4):677–686, 1999.

[4] J.-M. Bony. Solutions globales bornées pour les modèles discrets de l'équation de Boltzmann, en dimension 1 d'espace. In *Journées "Équations aux derivées partielles" (Saint Jean de Monts, 1987)*, pages Exp. No. XVI, 10. École Polytech., Palaiseau, 1987.

[5] David Borwein and Jonathan Borwein. Deriving new sinc results from old. *Amer. Math. Monthly*, 121(8):700–705, 2014.

[6] Torsten Carleman. Sur la théorie de l'équation intégrodifférentielle de Boltzmann. *Acta Math.*, 60(1):91–146, 1933.

[7] Carlo Cercignani, Reinhard Illner, and Mario Pulvirenti. *The mathematical theory of dilute gases*, volume 106 of *Applied Mathematical Sciences*. Springer-Verlag, New York, 1994.

[8] Ingrid Daubechies. *Ten lectures on wavelets*, volume 61 of *CBMS-NSF Regional Conference Series in Applied Mathematics*. Society for Industrial and Applied Mathematics (SIAM), Philadelphia, PA, 1992.

[9] Laura Fainsilber, Pär Kurlberg, and Bernt Wennberg. Lattice points on circles and discrete velocity models for the Boltzmann equation. *SIAM J. Math. Anal.*, 37(6):1903–1922 (electronic), 2006.

[10] Francis Filbet and Clément Mouhot. Analysis of spectral methods for the homogeneous Boltzmann equation. *Trans. Amer. Math. Soc.*, 363(4):1947–1980, 2011.

[11] Francis Filbet, Clément Mouhot, and Lorenzo Pareschi. Solving the Boltzmann equation in $N \log_2 N$. *SIAM J. Sci. Comput.*, 28(3):1029–1053 (electronic), 2006.

[12] I. M. Gamba, V. Panferov, and C. Villani. Upper Maxwellian bounds for the spatially homogeneous Boltzmann equation. *Arch. Ration. Mech. Anal.*, 194(1):253–282, 2009.

[13] Irene M. Gamba and Sri Harsha Tharkabhushanam. Spectral-Lagrangian methods for collisional models of non-equilibrium statistical states. *J. Comput. Phys.*, 228(6):2012–2036, 2009.

[14] Irene M. Gamba and Sri Harsha Tharkabhushanam. Shock and boundary structure formation by spectral-Lagrangian methods for the inhomogeneous Boltzmann transport equation. *J. Comput. Math.*, 28(4):430–460, 2010.

[15] Yves Meyer. *Wavelets*. Society for Industrial and Applied Mathematics (SIAM), Philadelphia, PA, 1993. Algorithms & applications, Translated from the French and with a foreword by Robert D. Ryan.

[16] Stéphane Mischler. Convergence of discrete-velocity schemes for the Boltzmann equation. *Arch. Rational Mech. Anal.*, 140(1):53–77, 1997.

[17] Stéphane Mischler and Bernt Wennberg. On the spatially homogeneous Boltzmann equation. *Ann. Inst. H. Poincaré Anal. Non Linéaire*, 16(4):467–501, 1999.

[18] Clément Mouhot and Cédric Villani. Regularity theory for the spatially homogeneous Boltzmann equation with cut-off. *Arch. Ration. Mech. Anal.*, 173(2):169–212, 2004.

[19] Andrzej Palczewski and Jacques Schneider. Existence, stability, and convergence of solutions of discrete velocity models to the Boltzmann equation. *J. Statist. Phys.*, 91(1-2):307–326, 1998.

[20] Vladislav A. Panferov and Alexei G. Heintz. A new consistent discrete-velocity model for the Boltzmann equation. *Math. Methods Appl. Sci.*, 25(7):571–593, 2002.

[21] Lorenzo Pareschi and Benoit Perthame. A Fourier spectral method for homogeneous Boltzmann equations. In *Proceedings of the Second*

International Workshop on Nonlinear Kinetic Theories and Mathematical Aspects of Hyperbolic Systems (Sanremo, 1994), volume 25, pages 369–382, 1996.

[22] Lorenzo Pareschi and Giovanni Russo. Numerical solution of the Boltzmann equation. I. Spectrally accurate approximation of the collision operator. *SIAM J. Numer. Anal.*, 37(4):1217–1245, 2000.

[23] Lorenzo Pareschi and Giovanni Russo. On the stability of spectral methods for the homogeneous Boltzmann equation. In *Proceedings of the Fifth International Workshop on Mathematical Aspects of Fluid and Plasma Dynamics (Maui, HI, 1998)*, volume 29, pages 431–447, 2000.

[24] Ada Pulvirenti and Bernt Wennberg. A Maxwellian lower bound for solutions to the Boltzmann equation. *Comm. Math. Phys.*, 183(1):145–160, 1997.

[25] Minh-Binh Tran. Nonlinear approximation theory for the homogeneous Boltzmann equation I. *Submitted*.

[26] Minh-Binh Tran. Nonlinear approximation theory for the homogeneous Boltzmann equation II. *Submitted*.

[27] Cédric Villani. A review of mathematical topics in collisional kinetic theory. In *Handbook of mathematical fluid dynamics, Vol. I*, pages 71–305. North-Holland, Amsterdam, 2002.

[28] Chuanming Zong. *The cube: a window to convex and discrete geometry*, volume 168 of *Cambridge Tracts in Mathematics*. Cambridge University Press, Cambridge, 2006.